Radiative decays of h_c to the light mesons $\eta^{(\prime)}$: A perturbative QCD calculation

Chao-Jie Fan* and Jun-Kang He†

Institute of Particle Physics and Key Laboratory of Quark and Lepton Physics (MOE), Central China Normal University, Wuhan, Hubei 430079, P. R. China

(Received 28 May 2019; published 8 August 2019)

We study the radiative decays $h_c \to \gamma\eta^{(\prime)}$ in the framework of perturbative QCD and evaluate analytically the one-loop integrals with the light quark masses kept. Interestingly, the branching ratios $\mathcal{B}(h_c \to \gamma\eta^{(\prime)})$ are insensitive to both the light quark masses and the shapes of $\eta^{(\prime)}$ distribution amplitudes. And it is noticed that the contribution of the gluonic content of $\eta^{(\prime)}$ is almost equal to that of the quark-antiquark content of $\eta^{(\prime)}$ in the radiative decays $h_c \to \gamma\eta^{(\prime)}$. By employing the ratio $R_{h_c} = \mathcal{B}(h_c \to \gamma\eta)/\mathcal{B}(h_c \to \gamma\eta')$, we extract the mixing angle $\phi = 33.8° \pm 2.5°$, which is in clear disagreement with the Feldmann-Kroll-Stech result $\phi = 39.0° \pm 1.6°$ extracted from the ratio $R_{J/\psi}$ with nonperturbative matrix elements $\langle 0|G^a_{\mu\nu}\tilde{G}^{a,\mu\nu}|\eta^{(\prime)}\rangle$, but consistent with $\phi = 33.5° \pm 0.9°$ extracted from the asymptotic limit of the $\gamma^*\gamma - \eta'$ transition form factor and $\phi = 33.9° \pm 0.6°$ extracted from $R_{J/\psi}$ in perturbative QCD. We also briefly discuss possible reasons for the difference in the determinations of the mixing angle.

DOI: 10.1103/PhysRevD.100.034005

I. INTRODUCTION

In recent years, the radiative decays of charmonia to the light mesons $\eta^{(\prime)}$ have been revisited in various approaches, such as perturbative quantum chromodynamics (pQCD) [1–5] and phenomenological models [6–8] (see [5] and references therein for more details), since they are closely related to the issue of $\eta - \eta'$ mixing, which is important ingredient for understanding many interesting phenomena related to $\eta^{(\prime)}$. In Ref. [5], the processes $J/\psi \to \gamma\eta^{(\prime)}$ were investigated and the $R_{J/\psi} = \mathcal{B}(J/\psi \to \gamma\eta')/\mathcal{B}(J/\psi \to \gamma\eta)$ was used as the main input to extract the mixing angle $\phi = 33.9° \pm 0.6°$, which is in excellent agreement with the value $\phi = 33.5° \pm 0.9°$ [9] extracted from the asymptotic limit of the $\gamma^*\gamma - \eta'$ transition form factor (TFF) at $Q^2 \to +\infty$, but in clear disagreement with the Feldmann-Kroll-Stech (FKS) result $\phi = 39.0° \pm 1.6°$ [10] extracted from the ratio $R_{J/\psi}$ with nonperturbative matrix elements $\langle 0|G^a_{\mu\nu}\tilde{G}^{a,\mu\nu}|\eta^{(\prime)}\rangle$. The difference may arise from the $g^*g^* - \eta^{(\prime)}$ TFF used in the Ref. [5], in like manner, the $\gamma^*\gamma - \eta'$ TFF used in Ref. [9]. Anyhow, more investigations are needed to provide a better understanding of the $\eta - \eta'$ mixing.

*fancj@mails.ccnu.edu.cn
†hejk@mails.ccnu.edu.cn

Recently, the branching ratios of $h_c \to \gamma\eta'$ and $h_c \to \gamma\eta$ are first measured to be, respectively, $(1.52 \pm 0.27 \pm 0.29) \times 10^{-3}$ and $(4.7 \pm 1.5 \pm 1.4) \times 10^{-4}$ with a statistical significance of 8.4σ and 4.0σ by the BESIII Collaboration [11], where h_c is assigned as P-wave charmonium state with the quantum numbers $J^{PC} = 1^{+-}$ [12]. In the literature, there are fewer studies on the exclusive radiative decays $h_c \to \gamma\eta^{(\prime)}$ [13,14]. In Ref. [13], Zhu and Dai investigated these channels in the nonrelativistic QCD, where the contributions from the color-octet state of h_c are suppressed by a relative factor $v^2_{c\bar{c}}\alpha_s$. And they adopted the result of the Buchmuller-Tye potential model [15,16] for the value of the nonperturbative matrix elements, which can be directly related to the derivative of the nonrelativistic wave function at the origin [17]. While, for η' production, they evaluated the contributions from the gluonic content of η' by the TFF $F^{(g)}_{\eta' g^* g^*}$ [18]. However, in fact, the TFF $F^{(g)}_{\eta' g^* g^*}$ enters the decay amplitude of $h_c \to \gamma\eta'$ from one-loop processes. It means that Zhu and Dai [13] missed the leading order contributions of the gluonic content of η', which come from the tree level processes. Besides the QCD approach, Wu *et al.* studied the two decay processes with an intermediate meson loops model [14], and their predictions were compatible with the experimental measurements [11].

From a general point of view [19–26], the decays of heavy quarkonium can be assumed that the annihilation of the heavy quark and antiquark is a short-distance process which can be described by perturbation theory, while the nonperturbative effect of the bound state could be factorized into its Bethe-Salpeter (B-S) wave function. In this work, we investigate the radiative decays $h_c \to \gamma\eta^{(\prime)}$ in the framework of pQCD and take a nonrelativistic quark model with the zero-binding approximation for the initial bound state h_c. For the final light mesons $\eta^{(\prime)}$, because of the large momentum transfer, light-cone distribution amplitudes (DAs) are adopted. As mentioned above, the issue of $\eta-\eta'$ mixing is also involved in the decays $h_c \to \gamma\eta^{(\prime)}$, and we address this issue along the same line as Ref. [5].

In this paper, we present a detailed calculation of the radiative decays $h_c \to \gamma\eta^{(\prime)}$. The involved five-point and four-point one-loop integrals are decomposed into a sum of three-point integrals and then evaluated analytically with the light quark masses kept. The branching ratios $\mathcal{B}(h_c \to \gamma\eta^{(\prime)})$ are found to be insensitive to the light quark masses and the shapes of the light meson DAs, which are in accord with the situation in the decay processes $J/\psi \to \gamma\eta^{(\prime)}$ [5]. And our numerical results show that the contributions from the gluonic content of $\eta^{(\prime)}$ and those from quark-antiquark content of $\eta^{(\prime)}$ are comparable with each other. The possible reasons are that first, the quark-antiquark contributions are Okubo-Zweig-Iizuka (OZI) suppressed. Specifically, the quark-antiquark contributions, which come from the one-loop OZI-forbidden processes, are suppressed by the factor α_s as compared with the gluonic contributions in the decay amplitudes. Second, the gluonic DA of $\eta^{(\prime)}$ can mix with their quark-antiquark DA under the QCD evolution due to the $U_A(1)$ anomaly [27], which makes the gluonic part of the $\eta^{(\prime)}$ wave functions be not negligible at the charmonium scale. In addition, we should note that in the radiative decays $J/\psi \to \gamma\eta^{(\prime)}$ [1,5,28], the gluonic contributions are strongly suppressed by the factor $m^2_{\eta^{(\prime)}}/M^2_{J/\psi}$ because of the spin structure of their amplitudes. While similar suppressions do not exist in the decays $h_c \to \gamma\eta^{(\prime)}$.

The paper is organized as follows. The formalism for the decay processes $h_c \to \gamma\eta^{(\prime)}$ is presented in Sec. II. In Sec. III, we present our numerical results while Sec. IV is our summary. The expressions of the 11 numerators introduced in Sec. II are given in the Appendix.

II. THE RADIATIVE DECAYS $h_c \to \gamma\eta^{(\prime)}$ IN PQCD

A. The contributions of the quark-antiquark content of $\eta^{(\prime)}$

For the quark-antiquark content of $\eta^{(\prime)}$, the leading order contributions to the radiative decays $h_c \to \gamma\eta^{(\prime)}$ come from one-loop processes, and one of the corresponding Feynman diagrams is depicted in Fig. 1. There are other five diagrams from permutations of the photon and gluon legs. Following the procedure given in Ref. [25], it is convenient to divide the covariant amplitude of $h_c \to \gamma\eta^{(\prime)}$ into two independent amplitudes. One amplitude describes the effective coupling between h_c, a real photon, and two virtual gluons, and the other describes the effective coupling between $\eta^{(\prime)}$ and two

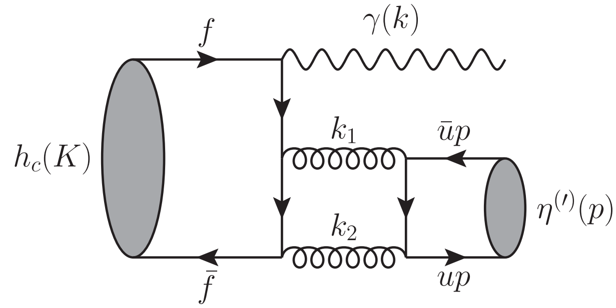

FIG. 1. One typical Feynman diagram for $h_c \to \gamma\eta^{(\prime)}$ with the quark-antiquark content of $\eta^{(\prime)}$. Here kinematical variables are labeled.

virtual gluons. Then the amplitude of $h_c \to \gamma\eta^{(\prime)}$ can be obtained by multiplying the two amplitudes, inserting the gluon propagators and performing the loop integration.

In the rest frame of h_c, the amplitude of $h_c \to \gamma g^* g^*$ can be given by [29]

$$A = A^{\alpha\beta\mu\nu}\varepsilon_\alpha(K)\epsilon^*_\beta(k)\epsilon^*_\mu(k_1)\epsilon^*_\nu(k_2) = \sqrt{3}\int\frac{d^4q_c}{(2\pi)^4}\mathrm{Tr}[\chi(K,q_c)\hat{\mathcal{O}}(q_c)], \tag{1}$$

where $\chi(K,q_c)$ is the B-S wave function of h_c and $\hat{\mathcal{O}}(q_c)$ is the hard-scattering amplitude. Here the factor $\sqrt{3}$ is included to account for the color properties of the quark and antiquark. K, k, k_1, k_2, and $\varepsilon(K)$, $\epsilon(k)$, $\epsilon(k_1)$, $\epsilon(k_2)$ are the momenta and polarization vectors of the h_c, the photon, and the two gluons, respectively. The momenta of the quark c and antiquark $\bar{c}$ have the form

$$f = \frac{K}{2} + q_c, \qquad \bar{f} = \frac{K}{2} - q_c, \tag{2}$$

with q_c the relative momentum between the quark c and antiquark $\bar{c}$. In a nonrelativistic bound state picture, the B-S wave function $\chi(K,q_c)$ can be reduced to its nonrelativistic form [30,31],

$$\chi(K,q_c) = 2\pi\delta(q_c^0)\psi_{1m}(\boldsymbol{q_c})\mathcal{P}(K,q_c), \tag{3}$$

where $\psi_{1m}(\boldsymbol{q_c})$ is the bound state wave function of P-wave charmonium h_c. The spin projection operator $\mathcal{P}(K,q_c)$ can be written in a covariant form [31]

$$\mathcal{P}(K,q_c) = \sqrt{\frac{1}{8m_c^3}}\left(m_c + \frac{\not{K}}{2} + \not{q}_c\right)(-\gamma^5)\left(m_c - \frac{\not{K}}{2} + \not{q}_c\right), \tag{4}$$

with m_c the c quark mass. Since the wave function $\psi_{1m}(\boldsymbol{q_c})$ is sharply damped for relative momenta which become large at the scale of the h_c mass, one can expand the

$\mathrm{Tr}[\mathcal{P}(K,q_c)\hat{\mathcal{O}}(q_c)]$ to the first order in q_c for the P-wave charmonium h_c. Then the amplitude can be rewritten as

$$A=\sqrt{3}\int\frac{\mathrm{d}^3q_c}{(2\pi)^3}\psi_{1m}(\boldsymbol{q_c})q_c^\alpha \times\mathrm{Tr}[\mathcal{P}_\alpha(K,0)\hat{\mathcal{O}}(0)+\mathcal{P}(K,0)\hat{\mathcal{O}}_\alpha(0)], \tag{5}$$

where

$$\mathcal{P}_\alpha(K,0)=\frac{\partial}{\partial q_c^\alpha}\mathcal{P}(K,q_c)\Big|_{q_c=0},\quad \hat{\mathcal{O}}_\alpha(0)=\frac{\partial}{\partial q_c^\alpha}\hat{\mathcal{O}}(q_c)\Big|_{q_c=0}. \tag{6}$$

With the zero-binding approximation [30,31], one can obtain

$$A=\sqrt{3}\left(-i\sqrt{\frac{3}{4\pi}}R'_{h_c}(0)\right)\varepsilon^\alpha(K) \times\mathrm{Tr}[\mathcal{P}_\alpha(K,0)\hat{\mathcal{O}}(0)+\mathcal{P}(K,0)\hat{\mathcal{O}}_\alpha(0)], \tag{7}$$

where $R'_{h_c}(0)$ denotes the derivative of the radial wave function of h_c evaluated at the origin

$$\int\frac{\mathrm{d}^3q_c}{(2\pi)^3}\psi_{1m}(\boldsymbol{q_c})q_c^\alpha=-i\sqrt{\frac{3}{4\pi}}R'_{h_c}(0)\varepsilon^\alpha(K). \tag{8}$$

Taking the nonrelativistic approximation $m_c\approx M/2$, one can obtain

$$\mathcal{P}(K,0)=\sqrt{\frac{1}{4M}}(\not{K}+M)(-\gamma^5),$$
$$\mathcal{P}^\alpha(K,0)=\sqrt{\frac{1}{M}}\frac{\gamma^\alpha\not{K}}{M}(-\gamma^5), \tag{9}$$

and

$$\hat{\mathcal{O}}(0)=Q_c\sqrt{4\pi\alpha}(4\pi\alpha_s)\frac{\delta_{ab}}{6}\frac{i}{4}\left[\not{\epsilon}^*(k_2)\frac{\not{k}_2-\not{k}_1-\not{k}+M}{(k_1+k)\cdot k_2}\not{\epsilon}^*(k)\frac{\not{k}_2+\not{k}-\not{k}_1+M}{(k_2+k)\cdot k_1}\not{\epsilon}^*(k_1)+(5\text{ permutations of }k_1,k_2\text{ and }k)\right],$$
$$\hat{\mathcal{O}}^\alpha(0)=Q_c\sqrt{4\pi\alpha}(4\pi\alpha_s)\frac{\delta_{ab}}{6}\frac{i}{4}\left[\not{\epsilon}^*(k_2)\frac{2\gamma^\alpha}{(k_1+k)\cdot k_2}\not{\epsilon}^*(k)\frac{\not{k}_2+\not{k}-\not{k}_1+M}{(k+k_2)\cdot k_1}\not{\epsilon}^*(k_1)\right.$$
$$+\not{\epsilon}^*(k_2)\frac{(k_2-k-k_1)^\alpha(\not{k}_2-\not{k}-\not{k}_1+M)}{[(k_1+k\cdot k_2)\cdot k_2]^2}\not{\epsilon}^*(k)\frac{\not{k}_2+\not{k}-\not{k}_1+M}{(k+\cdot k_2)\cdot k_1}\not{\epsilon}^*(k_1)$$
$$+\not{\epsilon}^*(k_2)\frac{\not{k}_2-\not{k}_1-\not{k}+M}{(k_1+k)\cdot k_2}\not{\epsilon}^*(k)\frac{(k_2+k-k_1)^\alpha(\not{k}_2+\not{k}-\not{k}_1+M)}{[(k+k_2)\cdot k_1]^2}\not{\epsilon}^*(k_1)$$
$$\left.+\not{\epsilon}^*(k_2)\frac{\not{k}_2-\not{k}_1-\not{k}+M}{(k_1+k)\cdot k_2}\not{\epsilon}^*(k)\frac{2\gamma^\alpha}{(k+k_2)\cdot k_1}\not{\epsilon}^*(k_1)+(5\text{ permutations of }k_1,k_2\text{ and }k)\right]. \tag{10}$$

At the leading twist level, the light-cone matrix elements of the quark-antiquark content of $\eta^{(\prime)}$ are given by [32]

$$\langle\eta^{(\prime)}(p)|\bar{q}_\alpha(x)q_\beta(y)|0\rangle =\frac{i}{4}f^q_{\eta^{(\prime)}}(\not{p}\gamma_5)_{\beta\alpha}\int\mathrm{d}ue^{i(up\cdot x+\bar{u}p\cdot y)}\phi^q(u),\qquad(q=u,d,s), \tag{11}$$

where the decay constants $f^q_{\eta^{(\prime)}}$ are defined as

$$\langle0|\bar{q}(0)\gamma_\mu\gamma_5q(0)|\eta^{(\prime)}(p)\rangle=if^q_{\eta^{(\prime)}}p_\mu. \tag{12}$$

Following the conventions in Refs. [2,18,33–35], the $g^*g^*-\eta^{(\prime)}$ TFFs can be parametrized as

$$\mathcal{M}_{\mu\nu}=-i(4\pi\alpha_s)\delta_{ab}\epsilon_{\mu\nu\rho\sigma}k_1^\rho k_2^\sigma F_{g^*g^*-\eta^{(\prime)}}(k_1^2,k_2^2), \tag{13}$$

and the TFFs $F_{g^*g^*-\eta^{(\prime)}}(k_1^2,k_2^2)$ read

$$F_{g^*g^*-\eta^{(\prime)}}(k_1^2,k_2^2) =\frac{1}{6}\sum_{q=u,d,s}f^q_{\eta^{(\prime)}}\int_0^1\mathrm{d}u\phi^q(u,\mu) \times\left(\frac{1}{\bar{u}k_1^2+uk_2^2-u\bar{u}m^2_{\eta^{(\prime)}}-m_q^2+i\epsilon}+(u\leftrightarrow\bar{u})\right), \tag{14}$$

where $\bar{u}=1-u$, u is the momentum fraction carried by the quark, and m_q is the mass of the quark ($q=u$, d, s). And the light-cone DA has the form [36]

$$\phi^q(u)=6u(1-u)\left(1+\sum_{n=2,4\cdots}c_n^q(\mu)C_n^{\frac{3}{2}}(2u-1)\right), \tag{15}$$

TABLE I. Gegenbauer coefficients of three sample models with the scale $\mu_0 = 1$ GeV.

Model	$c_2^q(\mu_0)$	$c_4^q(\mu_0)$	$c_2^g(\mu_0)$
I	0.10	0.10	−0.26
II	0.20	0.00	−0.31
III	0.25	−0.10	−0.25

with $c_n^q(\mu)$ the Gegenbauer moments. In Table I, we list the three models of the DAs discussed in Ref. [36]. The shapes of the corresponding DAs are shown in Fig. 2, where the $c_n^q(\mu)$ are evaluated at the scale $\mu = M/2$.

As mentioned above, one can obtain the amplitude of $h_c \to \gamma\eta^{(\prime)}$ by multiplying the two part amplitudes, inserting the gluon propagators, and integrating over the loop momentum,

$$M_T = T^{\alpha\beta}\varepsilon_\alpha(K)\epsilon_\beta^*(k) = \frac{1}{2}\int\frac{\mathrm{d}^4k_1}{(2\pi)^4}A^{\alpha\beta\mu\nu}M_{\mu\nu}\varepsilon_\alpha(K)\epsilon_\beta^*(k)\frac{i}{k_1^2+i\epsilon}\frac{i}{k_2^2+i\epsilon}, \quad (16)$$

where the factor $\frac{1}{2}$ takes into account that the two gluons have already been interchanged both in $A^{\alpha\lambda\mu\nu}$ and $M_{\mu\nu}$. Using parity conservation, Lorentz invariance, and gauge invariance, one can prove that

$$T^{\alpha\beta} \sim \left(-g^{\alpha\beta} + \frac{k^\alpha K^\beta}{k\cdot K}\right), \quad (17)$$

i.e., there is only one independent helicity amplitude H^q_{QCD} [25],

$$T^{\alpha\beta} = H^q_{\mathrm{QCD}} h^{\alpha\beta}, \quad (18)$$

where

$$h^{\alpha\beta} = \left(-g^{\alpha\beta} + \frac{k^\alpha K^\beta}{k\cdot K}\right). \quad (19)$$

With the help of the helicity projector [25]

$$\mathbb{P}^{\alpha\beta} = \frac{1}{2}h_{\alpha'\beta'}\left(-g^{\alpha\alpha'} + \frac{K^\alpha K^{\alpha'}}{M^2}\right)(-g^{\beta\beta'}) = \frac{1}{2}\left(-g^{\alpha\beta} + \frac{k^\alpha K^\beta}{k\cdot K}\right), \quad (20)$$

we obtain the helicity amplitude

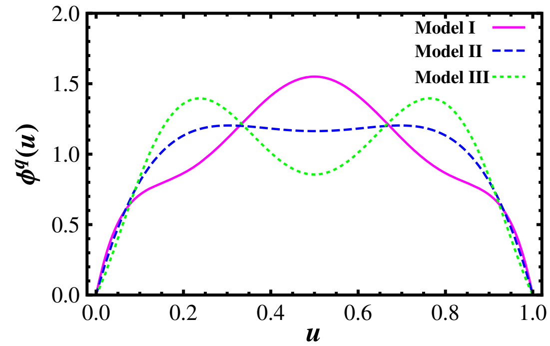

FIG. 2. The shapes of the corresponding DAs with the scale $\mu = M/2$.

$$H^q_{\mathrm{QCD}} = T^{\alpha\beta}\mathbb{P}_{\alpha\beta} = \frac{2Q_c}{3\sqrt{3}}\sqrt{4\pi\alpha}(4\pi\alpha_s)^2\left(-i\sqrt{\frac{3}{4\pi}}R'_{h_c}\right)\sum_{q=u,d,s}\frac{f^q_{\eta^{(\prime)}}}{M^{\frac{5}{2}}}H_q, \quad (21)$$

where the dimensionless function H_q reads

$$H_q = \frac{1}{16\pi^2}\int \mathrm{d}u\phi^q(u)I_q(u). \quad (22)$$

$I_q(u)$ is the summation of the loop integrals of the six Feynman diagrams,

$$I_q(u) = \frac{1}{i\pi^2}\int \mathrm{d}^4l\left(\frac{N_1}{D_1D_2^2D_3D_4D_5} + \frac{N_2}{D_1D_2D_3^2D_4D_5} + \frac{N_3}{D_1D_2^2D_4D_5} + \frac{N_4}{D_1D_3^2D_4D_5} + \frac{N_5}{D_1D_2D_3D_4D_5} + \frac{N_6}{D_1D_2D_4D_5} + \frac{N_7}{D_1D_3D_4D_5}\right) + (u \leftrightarrow \bar{u}), \quad (23)$$

with $l = k_1 - k_2$. Here the expressions of the denominators are given by

$$\begin{aligned} D_1 &= (l+\xi p)^2 - 4m_q^2 + i\epsilon, \\ D_2 &= (l-k)^2 - M^2 + i\epsilon, \\ D_3 &= (l+k)^2 - M^2 + i\epsilon, \\ D_4 &= (l+p)^2 + i\epsilon, \\ D_5 &= (l-p)^2 + i\epsilon, \end{aligned} \quad (24)$$

and the seven numerators N_i ($i = 1$–7) read

$$\begin{aligned}
N_1 &= 32(1+x)M^4l^4 + 32M^2\bigg[(3x-1)M^4 - M^2(2l\cdot k + (1-x)l\cdot p)\\
&\quad - 2l\cdot K\left(\frac{2(1+x)}{1-x}l\cdot k + l\cdot p\right)\bigg]l^2 - 32\bigg[M^6(2xl\cdot k - (1-x)l\cdot p)\\
&\quad - 2M^4\left(3l\cdot kl\cdot p - \frac{4x(l\cdot k)^2}{1-x} - (l\cdot p)^2\right) - 4l\cdot kl\cdot pl\cdot K\left(M^2 + \frac{2l\cdot K}{1-x}\right)\bigg],\\
N_2 &= 32(1+x)M^4l^4 + 32M^2\bigg[(3x-1)M^4 + M^2(2l\cdot k + (1-x)l\cdot p)\\
&\quad - 2l\cdot K\left(\frac{2(1+x)}{1-x}l\cdot k + l\cdot p\right)\bigg]l^2 + 32\bigg[M^6(2xl\cdot k - (1-x)l\cdot p)\\
&\quad + 2M^4\left(3l\cdot kl\cdot p - \frac{4x(l\cdot k)^2}{1-x} - (l\cdot p)^2\right) - 4l\cdot kl\cdot pl\cdot K\left(M^2 - \frac{2l\cdot K}{1-x}\right)\bigg],\\
N_3 &= 32M^2\left[(1+x)M^2 - \frac{2xl\cdot p}{1-x} + \left(\frac{1+x}{1-x}\right)^2 l\cdot k\right]l^2 - 64\left(M^2 + \frac{2l\cdot p}{(1-x)^2} + \frac{l\cdot k}{1-x}\right)l\cdot pl\cdot k\\
&\quad - 16\left[2xM^4l\cdot k - (1-x)M^4l\cdot p + 4M^2(l\cdot p)^2 - \frac{4(l\cdot p)^3}{1-x}\right],\\
N_4 &= 32M^2\left[(1+x)M^2 + \frac{2xl\cdot p}{1-x} - \left(\frac{1+x}{1-x}\right)^2 l\cdot k\right]l^2 - 64\left(M^2 - \frac{2l\cdot p}{(1-x)^2} - \frac{l\cdot k}{1-x}\right)l\cdot pl\cdot k\\
&\quad + 16\left[2xM^4l\cdot k - (1-x)M^4l\cdot p - 4M^2(l\cdot p)^2 - \frac{4(l\cdot p)^3}{1-x}\right],\\
N_5 &= -64M^2[(1+x)M^2l^2 - 2l\cdot pl\cdot K], \qquad N_6 = N_7 = \frac{32}{1-x}[(1+x)M^2l^2 - 2l\cdot pl\cdot K], \qquad (25)
\end{aligned}$$

with $x = m^2/M^2$ and $\xi = 1\text{–}2u$. Before going to calculate the integrals, it is useful and essential to present a short analysis of its IR properties. Obviously, when one of the gluons becomes soft, e.g., $l \to p$, the propagator denominators D_1 (with $u = 1 - m_q/m$), D_3, and D_5 tend to be zero, namely the individual integral may encounter soft singularities according to the conclusion in the Ref. [37]. However, for a given decay process, one need to go a step further and make an analysis of the numerator and denominator in the integrand simultaneously. When $l = p + \lambda$ (the λ is a small quantity), one can obtain the numerators

$$N_1 \sim N_2 \sim N_4 \sim \lambda^2, \qquad N_3 \sim N_5 \sim N_6 \sim N_7 \sim \lambda, \qquad (26)$$

and the on-shell propagator denominators

$$D_1 \sim D_3 \sim \lambda, \qquad D_5 \sim \lambda^2. \qquad (27)$$

For the ultrasoft gluon ($\lambda \to 0$), the contributions to the loop function $I_q(u)$ have the form

$$\begin{aligned}
&\int_{l=p+\lambda} \mathrm{d}^4l\bigg(\frac{N_1}{D_1D_2^2D_3D_4D_5} + \frac{N_2}{D_1D_2D_3^2D_4D_5} + \frac{N_3}{D_1D_2^2D_4D_5}\\
&\quad + \frac{N_4}{D_1D_3^2D_4D_5} + \frac{N_5}{D_1D_2D_3D_4D_5}\\
&\quad + \frac{N_6}{D_1D_2D_4D_5} + \frac{N_7}{D_1D_3D_4D_5}\bigg) \sim \int \mathrm{d}^4\lambda\frac{\lambda}{\lambda^4} \to 0. \qquad (28)
\end{aligned}$$

It means the loop function is IR safe in the potentially dangerous region.

By using the algebraic identities,

$$\begin{aligned}
&l\cdot k = \frac{D_3 - D_2}{4}, \qquad l\cdot p = \frac{D_4 - D_5}{4},\\
&l\cdot K = \frac{D_4 - D_5 + D_3 - D_2}{4}, \qquad (29)
\end{aligned}$$

and

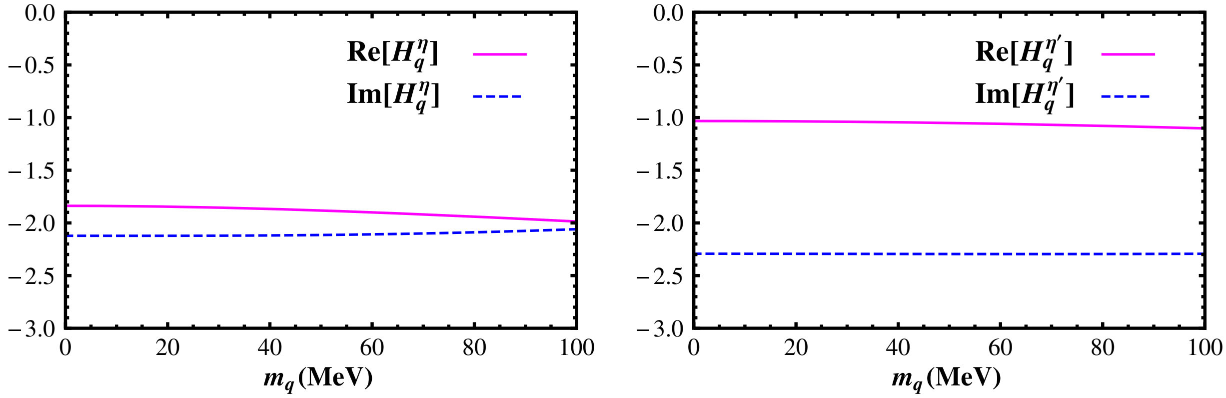

FIG. 3. The m_q dependence of real and imaginary parts of the dimensionless functions $H_q^{\eta'}$ and H_q^{η}.

$$
\begin{aligned}
M^2 &= \frac{D_4+D_5}{2(1+x)} - \frac{D_2+D_3}{2(1+x)},\\
M^2 &= -\frac{D_1}{(1-\xi^2)x+y} + \frac{(1+\xi)D_4}{2[(1-\xi^2)x+y]} + \frac{(1-\xi)D_5}{2[(1-\xi^2)x+y]},\\
l^2 &= \frac{D_4+D_5}{2(1+x)} + \frac{x(D_2+D_3)}{2(1+x)},\\
l^2 &= \frac{D_1}{1-\xi^2+\frac{y}{x}} - \frac{[\xi(1+\xi)-\frac{y}{x}]D_4}{2(1-\xi^2+\frac{y}{x})} + \frac{[\xi(1-\xi)+\frac{y}{x}]D_5}{2(1-\xi^2+\frac{y}{x})},
\end{aligned}
\tag{30}
$$

with $y = 4m_q^2/M^2$; the loop function $I_q(u)$ is decomposed into the sum of three-point one-loop integrals, which can be analytically calculated with the technique proposed in Ref. [38] or the computer program Package − X [39,40]. Performing the convolution integral between the loop function $I_q(u)$ and the DA $\phi^q(u)$, our results show that the dimensionless function H_q is insensitive to the light quark mass m_q. Specifically, the change of the absolute value of the dimensionless function H_q does not exceed 2% when the value of m_q varies in the range 0–100 MeV for all the three kinds of $\eta^{(\prime)}$ DAs in Fig. 2. As a consequence, the light quark mass can be neglected safely and reasonably. As shown schematically in Fig. 3, we present the light quark mass m_q dependence of the dimensionless functions $H_q^\eta = H_q|_{m=m_\eta}$ and $H_q^{\eta'} = H_q|_{m=m_{\eta'}}$ with the "narrow" DA (model I in Fig. 2). The property of the dimensionless function H_q is similar with that in the radiative decays $J/\psi \to \gamma\eta^{(\prime)}$ [5].

For showing the analytical expression of the loop function more clearly, we define

$$
\begin{aligned}
I_0(u) &= \lim_{m_q\to 0} I_q(u)\\
H_0 &= \frac{1}{16\pi^2}\int \mathrm{d}u\phi^q(u)I_0(u),
\end{aligned}
\tag{31}
$$

and then the helicity amplitude $H_{\rm QCD}^q$ in Eq. (21) can be simplified to

$$
H_{\rm QCD}^q = \frac{2Q_c}{3\sqrt{3}}\sqrt{4\pi\alpha}(4\pi\alpha_s)^2\left(-i\sqrt{\frac{3}{4\pi}}R'_{h_c}(0)\right)\frac{f_{\eta^{(\prime)}}}{M^{\frac{5}{2}}}H_0,
\tag{32}
$$

with the effective decay constants

$$
f_{\eta'} = f_{\eta'}^u + f_{\eta'}^d + f_{\eta'}^s, \qquad f_\eta = f_\eta^u + f_\eta^d + f_\eta^s.
\tag{33}
$$

Finally, we present a brief analysis about the loop function $I_0(u)$. Taking the substitution $l \to -l$, one can obtain

$$
D_2 \leftrightarrow D_3, \qquad D_4 \leftrightarrow D_5,
\tag{34}
$$

then the loop function $I_0(u)$ can be reduced to 11 one-loop integrals

$$
\begin{aligned}
I_0(u) = \frac{1}{i\pi^2}\int \mathrm{d}^4 l\bigg(&\frac{n_1}{D_1D_2^2D_3} + \frac{n_2}{D_1D_2^2D_4} + \frac{n_3}{D_1D_2^2D_5}\\
&+ \frac{n_4}{D_2^2D_3D_4} + \frac{n_5}{D_2^2D_3D_5} + \frac{n_6}{D_2^2D_4D_5}\\
&+ \frac{n_7}{D_1D_2D_3} + \frac{n_8}{D_1D_2D_4} + \frac{n_9}{D_1D_2D_5}\\
&+ \frac{n_{10}}{D_2D_3D_4} + \frac{n_{11}}{D_2D_4D_5}\bigg) + (u \leftrightarrow \bar{u}),
\end{aligned}
\tag{35}
$$

and the expressions of the 11 numerators n_i $(i = 1 \sim 11)$ are given in the Appendix. It is noticed that the loop functions $I_0^\eta(u) = I_0(u)|_{m=m_\eta}$ and $I_0^{\eta'}(u) = I_0(u)|_{m=m_{\eta'}}$ are quite steady over the most region of u as shown in Fig. 4. Consequently, the convolution integral between the loop function $I_0(u)$ and the DA becomes insensitive to the shape of the final meson DA—in other words, it almost becomes the normalization of the DA. Specifically, the change among the dimensionless function H_0 with the different models of the DAs in Fig. 2 is less than 2%.

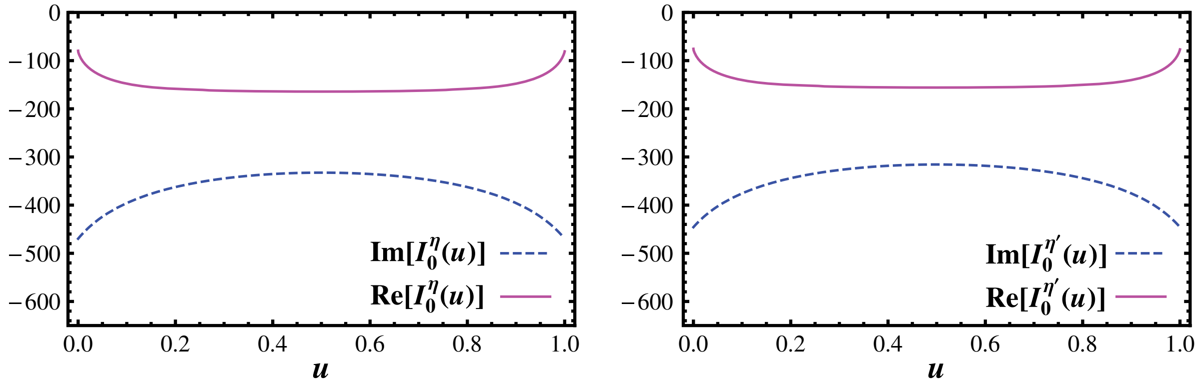

FIG. 4. The u dependence of real and imaginary parts of the loop functions $I_0^\eta(u)$ and $I_0^{\eta'}(u)$.

B. The contributions of the gluonic content of $\eta^{(\prime)}$

For the gluonic content of $\eta^{(\prime)}$, the leading order contributions to the radiative decays $h_c \to \gamma\eta^{(\prime)}$ come from the tree level processes. One of the Feynman diagrams is shown in Fig. 5, and the other two diagrams arise from permutations of the photon and gluon legs.

The leading twist in the light-cone expansion of the matrix elements of the meson $\eta^{(\prime)}$ over two-gluon fields is [27,32,36]

$$\langle \eta^{(\prime)}(p)|A^a_\alpha(x)A^b_\beta(y)|0\rangle = \frac{1}{4}\epsilon_{\alpha\beta\rho\sigma}\frac{k^\rho p^\sigma}{p\cdot k}\frac{C_F}{\sqrt{3}}\frac{\delta^{ab}}{8}f^1_{\eta^{(\prime)}}\int \mathrm{d}u e^{i(up\cdot x+\bar{u}p\cdot y)}\frac{\phi^g(u)}{u(1-u)}, \tag{36}$$

with the effective decay constant $f^1_{\eta^{(\prime)}} = \frac{1}{\sqrt{3}}(f^u_{\eta^{(\prime)}} + f^d_{\eta^{(\prime)}} + f^s_{\eta^{(\prime)}})$ and the gluonic twist-2 DA [32,36,41],

$$\phi^g(u) = 30u^2(1-u)^2\sum_{n=2,4\cdots} c^g_n(\mu)C^{\frac{5}{2}}_{n-1}(2u-1). \tag{37}$$

Then we can obtain the corresponding helicity amplitude

$$H^g_{\mathrm{QCD}} = \frac{2Q_c}{9}\sqrt{4\pi\alpha}(4\pi\alpha_s)\left(-i\sqrt{\frac{3}{4\pi}}R'_{h_c}(0)\right)\frac{f^1_{\eta^{(\prime)}}}{M^{\frac{5}{2}}}H_g, \tag{38}$$

with

$$H_g = \int \mathrm{d}u\frac{\phi^g(u)}{u(1-u)}\frac{4(2u-1)(2ux(1-u)-x+1)}{u(1-u)(1-x^2(2u-1)^2)}. \tag{39}$$

Generally, the contributions of the gluonic content are expected to be small, since the gluonic content can be seen as the higher-order effects from the point of view of the QCD evolution of the gluon DA, which vanishes in the asymptotic limit. However, due to the $U_A(1)$ anomaly, the gluonic DA of $\eta^{(\prime)}$ can mix with their quark-antiquark DA, which makes the contributions of the gluonic content become important in the $\eta^{(\prime)}$ production. Moreover, unlike the situation in the radiative decays $J/\psi \to \gamma\eta^{(\prime)}$ [1,5,28], in which the contributions of the gluonic content are strongly suppressed by a factor $x = m^2/M^2$, there is no additional suppression factor in the decay processes $h_c \to \gamma\eta^{(\prime)}$, i.e., the gluonic content of $\eta^{(\prime)}$ may play an important role in $h_c \to \gamma\eta^{(\prime)}$.

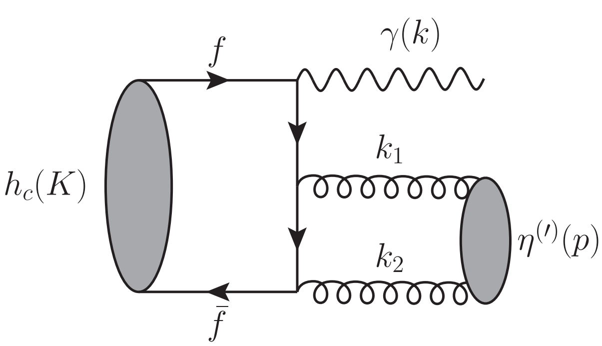

FIG. 5. One typical Feynman diagram for $h_c \to \gamma\eta^{(\prime)}$ with the gluonic content of $\eta^{(\prime)}$. Here kinematical variables are labeled.

III. NUMERICAL RESULTS

In the rest frame of h_c, the decay width of $h_c \to \gamma\eta^{(\prime)}$ can be given by

$$\Gamma(h_c \to \gamma\eta^{(\prime)}) = \frac{2}{3}\frac{1-x}{16\pi M}|H^q_{\mathrm{QCD}} + H^g_{\mathrm{QCD}}|^2. \tag{40}$$

In the numerical calculations, we employ the data given by the Particle Data Group [12]: $M = 3525$ MeV, $m_\eta = 548$ MeV, $m_{\eta'} = 958$ MeV, $\Gamma_{h_c} = (0.70\pm0.28\pm0.22)$ MeV, and the decay constant $f_\pi = 130.2$ MeV. The strong coupling constant $\alpha_s(M/2) = 0.32$, which is calculated through the two-loop renormalization group equation. For the derivative of the radial wave function of h_c evaluated at the origin $R'_{h_c}(0)$, we adopt the result of the Cornell potential model [16,42,43]

TABLE II. The values of ϕ, f_q, and f_s obtained with three phenomenological models [9,46].

	ϕ°	f_q/f_π	f_s/f_π
LEPs [46]	40.6 ± 0.9	1.10 ± 0.03	1.66 ± 0.06
ηTFF [9]	40.3 ± 1.8	1.06 ± 0.01	1.56 ± 0.24
η'TFF [9]	33.5 ± 0.9	1.09 ± 0.02	0.96 ± 0.04

$$|R'_{h_c}(0)|^2 = 0.131 \times 10^{15}\ \mathrm{MeV}^5. \tag{41}$$

For the Gegenbauer moments $c_2^q(\mu)$, $c_4^q(\mu)$, there are still large uncertainties as depicted in Table I. Fortunately, the dimensionless function H_0 in Eq. (31) is insensitive to the shapes of the $\eta^{(\prime)}$ DAs as we have shown in Sec. II. So in the following numerical calculations, we choose model I in Table I for the DA with the scale $\mu = M/2$.

For $\eta - \eta'$ system, the physical states $|\eta^{(\prime)}\rangle$ are usually treated as the mixing of the flavor states $|\eta_q\rangle = 1/\sqrt{2}|u\bar{u} + d\bar{d}\rangle$ and $|\eta_s\rangle = |s\bar{s}\rangle$ because of the $U_A(1)$ anomaly. As a manifestation of the celebrated OZI rule, one mixing angle is included in the flavor basis, and more details could be found in Refs. [10,36]. This is the known FKS scheme [10,44,45], in which the decay constants are parametrized as

$$f_\eta^u = f_\eta^d = \frac{f_q}{\sqrt{2}}\cos\phi, \qquad f_\eta^s = -f_s \sin\phi,$$
$$f_{\eta'}^u = f_{\eta'}^d = \frac{f_q}{\sqrt{2}}\sin\phi, \qquad f_{\eta'}^s = f_s \cos\phi. \tag{42}$$

Here the following definitions have been used [10,44,45]:

$$\langle 0|J_{\mu 5}^q(0)|\eta_q(p)\rangle = i f_q p_\mu, \quad \langle 0|J_{\mu 5}^q(0)|\eta_s(p)\rangle = 0,$$
$$\langle 0|J_{\mu 5}^s(0)|\eta_s(p)\rangle = i f_s p_\mu, \quad \langle 0|J_{\mu 5}^s(0)|\eta_q(p)\rangle = 0, \tag{43}$$

with the currents $J_{\mu 5}^q = 1/\sqrt{2}(\bar{u}\gamma_\mu\gamma_5 u + \bar{d}\gamma_\mu\gamma_5 d)$ and $J_{\mu 5}^s = \bar{s}\gamma_\mu\gamma_5 s$. The mixing angle ϕ and the decay constants f_q, f_s are three phenomenological parameters, which have been determined in different methods [9,10,46–48]. In Table II, we take the up-to-date values from Refs. [9,46]. The parameters extracted from the low energy processes (LEPs) $V \to \eta^{(\prime)}\gamma$, $\eta^{(\prime)} \to V\gamma$ ($V = \rho$, ω, ϕ) are listed in the first line. In the second line, the parameters are extracted with rational approximations for the η TFF $F_{\gamma^*\gamma\eta}(Q^2 \to +\infty)$. It is noteworthy that both the parameters in the first line and those in the second line are consistent with the FKS results [10]. While in the third line, the parameters are extracted with rational approximations for the η' TFF $F_{\gamma^*\gamma\eta'}(Q^2 \to +\infty)$, which is in accord with the *BABAR* measurements in the timelike region at $q^2 = 112\ \mathrm{GeV}^2$ [49].

For comparison, in Tables III and IV, we present the results with only the quark-antiquark contributions and those with only the gluonic contributions, respectively. Here $\Gamma_{h_c} = 0.70$ MeV is adopted. The branching ratios $\mathcal{B}(h_c \to \gamma\eta')$, $\mathcal{B}(h_c \to \gamma\eta)$ and their ratio $R_{h_c} = \mathcal{B}(h_c \to \gamma\eta)/\mathcal{B}(h_c \to \gamma\eta')$ are presented in the first, second, and third lines of the Tables III and IV, respectively. At first glance (Figs. 1 and 5), it seems that the branching ratios may be dominated by the "unsuppressed" tree level contributions from the gluonic content of $\eta^{(\prime)}$ (at order $\alpha\alpha_s^2$), rather than the one-loop contributions from the quark-antiquark content of $\eta^{(\prime)}$ (at order $\alpha\alpha_s^4$). However, from the two tables, one can find that the quark-antiquark content and the gluonic content of $\eta^{(\prime)}$ are of almost equal importance in the radiative decays $h_c \to \gamma\eta^{(\prime)}$.

In Table V, the results with the contributions from both the quark-antiquark content and the gluonic content are presented. Here we also adopt $\Gamma_{h_c} = 0.70$ MeV. From Table V, the branching ratios $\mathcal{B}(h_c \to \gamma\eta')$ and $\mathcal{B}(h_c \to \gamma\eta)$ are found to be greatly enhanced, because of the

TABLE III. The branching ratios $\mathcal{B}(h_c \to \gamma\eta^{(\prime)})$ with only the contributions of the quark-antiquark content.

	LEPs	ηTFF	η'TFF	Exp. [11]
$\mathcal{B}(h_c \to \gamma\eta')$	2.50×10^{-4}	2.26×10^{-4}	1.32×10^{-4}	$(1.52 \pm 0.27 \pm 0.29) \times 10^{-3}$
$\mathcal{B}(h_c \to \gamma\eta)$	6.5×10^{-7}	1.1×10^{-6}	3.6×10^{-5}	$(4.7 \pm 1.5 \pm 1.4) \times 10^{-4}$
R_{h_c}	0.3%	0.5%	27.5%	$(30.7 \pm 11.3 \pm 8.7)$%

TABLE IV. The branching ratios $\mathcal{B}(h_c \to \gamma\eta^{(\prime)})$ with only the contributions of the gluonic content.

	LEPs	ηTFF	η'TFF	Exp. [11]
$\mathcal{B}(h_c \to \gamma\eta')$	2.50×10^{-4}	2.26×10^{-4}	1.32×10^{-4}	$(1.52 \pm 0.27 \pm 0.29) \times 10^{-3}$
$\mathcal{B}(h_c \to \gamma\eta)$	5.6×10^{-7}	1.0×10^{-6}	3.1×10^{-5}	$(4.7 \pm 1.5 \pm 1.4) \times 10^{-4}$
R_{h_c}	0.2%	0.4%	23.8%	$(30.7 \pm 11.3 \pm 8.7)$%

TABLE V. The branching ratios $\mathcal{B}(h_c \to \gamma\eta^{(\prime)})$ with the contributions of both the quark-antiquark content and the gluonic content.

	LEPs	ηTFF	η'TFF	Exp. [11]
$\mathcal{B}(h_c \to \gamma\eta')$	7.06×10^{-4}	6.37×10^{-4}	3.73×10^{-4}	$(1.52\pm0.27\pm0.29)\times10^{-3}$
$\mathcal{B}(h_c \to \gamma\eta)$	2.0×10^{-6}	3.5×10^{-6}	1.1×10^{-4}	$(4.7\pm1.5\pm1.4)\times10^{-4}$
R_{h_c}	0.3%	0.6%	30.1%	$(30.7\pm11.3\pm8.7)\%$

constructive interference of the quark-antiquark contributions and the gluonic contributions. However, both $\mathcal{B}(h_c \to \gamma\eta')$ and $\mathcal{B}(h_c \to \gamma\eta)$ are still smaller than their experimental values. In addition, the ratio R_{h_c} can be comparable with its experimental value only with the η'TFF set of parameter values.

Considering the large uncertainties from the experimental measurement of the decay width Γ_{h_c} [50], the derivative of the radial wave function at the origin $R'_{h_c}(0)$ [16] and the factor $\alpha_s^4(\mu)$ involved in the branching ratios, it is very hard to give precise prediction for the individual branching ratio in practice. Even so, their ratio R_{h_c} could be predicted much more reliable, since the ratio R_{h_c} is independent of the decay width Γ_{h_c} and the derivative of the radial wave function at the origin $R'_{h_c}(0)$. Furthermore, the dependence of the ratio R_{h_c} on $\alpha_s(\mu)$ is also cut down to a large extent. So we are more interested in the ratio R_{h_c} rather than the individual branching ratio.

Without inputting any phenomenological parameters, we present a determination of the mixing angle ϕ by the ratio R_{h_c},

$$R_{h_c} = \frac{M^2 - m_\eta^2}{M^2 - m_{\eta'}^2} \frac{|H^q_{QCD} + H^g_{QCD}|^2_{m=m_\eta}}{|H^q_{QCD} + H^g_{QCD}|^2_{m=m_{\eta'}}}, \qquad (44)$$

and the ratio

$$\frac{\Gamma(\eta \to \gamma\gamma)}{\Gamma(\eta' \to \gamma\gamma)} = \frac{m_\eta^3}{m_{\eta'}^3} \left(\frac{5\sqrt{2}\frac{f_s}{f_q} - 2\tan\phi}{5\sqrt{2}\frac{f_s}{f_q}\tan\phi + 2} \right)^2. \qquad (45)$$

Employing the experimental data [11,12,51]

$$R_{h_c}^{\text{exp}} = (30.7 \pm 11.3 \pm 8.7)\%,$$
$$\Gamma^{\text{exp}}(\eta' \to \gamma\gamma) = 4.36(14)\ \text{KeV},$$
$$\Gamma^{\text{exp}}(\eta \to \gamma\gamma) = 0.516(18)\ \text{KeV}, \qquad (46)$$

one can obtain the mixing angle and the ratio f_s/f_q

$$\phi = 33.8° \pm 2.5°, \qquad \frac{f_s}{f_q} = 0.90 \pm 0.13, \qquad (47)$$

where the big uncertainty comes mainly from $R_{h_c}^{\text{exp}}$ [11]. Schematically, we show the dependence of the ratio R_{h_c} on the mixing angle ϕ in Fig. 6.

Obviously, the mixing angle ϕ determined by the ratio R_{h_c} is consistent with the η'TFF result $\phi = 33.5° \pm 0.9°$ [9], but in clear disagreement the FKS result $\phi = 39.0° \pm 1.6°$ extracted from the ratio $R_{J/\psi}$ with nonperturbative matrix elements $\langle 0|G^a_{\mu\nu}\tilde{G}^{a,\mu\nu}|\eta^{(\prime)}\rangle$ due to $U_A(1)$ anomaly dominance argument [10] and the LEPs result $\phi = 40.6° \pm 0.9°$ extracted from the low energy processes [46]. In lattice QCD, the UKQCD Collaboration [52] presented a value $\phi^{\text{fit}} \sim 34°$, while the ETM Collaboration [53] gave $\phi = 38.8° \pm 3.3°$. The difference in the determinations of the mixing angle ϕ may arise from the $g^*g^* - \eta^{(\prime)}$ TFF used in our calculation, in like manner, the $\gamma^*\gamma - \eta'$ TFF used in Ref. [9]. What is more interesting is that, in the same framework of pQCD, the mixing angles extracted from the ratio R_{h_c} ($\phi = 33.8° \pm 2.5°$) and the ratio $R_{J/\psi}$ ($\phi = 33.9° \pm 0.6°$) [5] are in excellent agreement with each other. In addition, the central value of the ratio f_s/f_q obtained in both this work and Refs. [5,9] is smaller than unity. While in the LEPs $V \to \eta^{(\prime)}\gamma$, $\eta^{(\prime)} \to V\gamma$ ($V = \rho$, ω, ϕ) [10,46], one usually predicted $f_s > f_q$, which is different from the result obtained in this work. However, from another point of view, the discrepancies in these determinations may indicate that our understanding of $\eta - \eta'$ mixing scheme is incomplete, and the physical picture of the $\eta - \eta'$ mixing at the high energy scale may differ from that at the low energy scale. Anyhow, the physics associated with the $\eta - \eta'$ mixing is interesting, and it is certainly worthy of further investigations for a

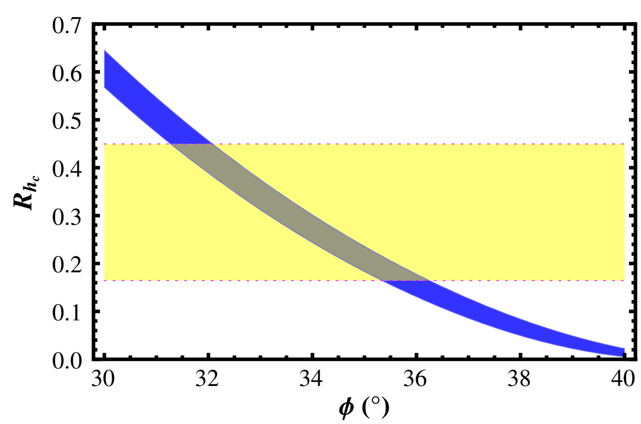

FIG. 6. The dependence of the ratio R_{h_c} on the mixing angle ϕ. The blue band is our calculated results with the uncertainties from the $\Gamma^{\text{exp}}(\eta^{(\prime)} \to \gamma\gamma)$. The yellow band denotes the experimental value of R_{h_c} with 1σ uncertainty.

better understanding of many phenomena in $\eta^{(\prime)}$ production processes.

IV. SUMMARY

In this work, we have calculated the branching ratios of the radiative decays $h_c \to \gamma\eta^{(\prime)}$ in the framework of pQCD. For the initial heavy quarkonium h_c, we neglected its internal momentum in a nonrelativistic picture. While the final light mesons $\eta^{(\prime)}$ are treated as a light-cone object, and we employ a set of DAs of the quark-antiquark content and those of the gluonic content as nonperturbative inputs. Using some algebraic identities, we decompose the five-point and four-point one-loop integrals into the three-point one-loop integrals and calculate these three-point one-loop integrals analytically. Our results of the branching ratios $\mathcal{B}(h_c \to \gamma\eta^{(\prime)})$ are insensitive to the light quark masses and the shapes of the $\eta^{(\prime)}$ DAs, which are similar to the situation in the decay processes $J/\psi \to \gamma\eta^{(\prime)}$ [5]. Furthermore, we find that the contributions from the quark-antiquark content are almost equal to those from the gluonic content, which are strongly suppressed in the heavy quarkonium decays $V \to \gamma\eta^{(\prime)}$ [1,5,28]. Interestingly enough, only with the set of ϕ, f_q, and f_s extracted from the asymptotic limit of the η' TFF, which is in accord with the *BABAR* measurement at $q^2 = 112\ \mathrm{GeV}^2$ [49], our result of the ratio R_{h_c} is comparable with its experimental data. As a crossing check, by using the R_{h_c}, $\Gamma(\eta^{(\prime)} \to \gamma\gamma)$ and their experimental values, we obtain the mixing angle $\phi = 33.8^\circ \pm 2.5^\circ$, which is in excellent consistent with the η'TFF result $\phi = 33.5^\circ \pm 0.9^\circ$ [9] and the result $\phi = 33.9^\circ \pm 0.6^\circ$ extracted by the ratio $R_{J/\psi}$ [5].

For the individual branching ratios $\mathcal{B}(h_c \to \gamma\eta')$ and $\mathcal{B}(h_c \to \gamma\eta)$, there are still considerable discrepancies between our results and the experimental measurements. The reason may be due to the sensitivity of the hard-scattering amplitude $\hat{\mathcal{O}}(q_c)$ to the internal momentum q_c in the P-wave decays, which can make the convergence of the q_c expansion of $\mathrm{Tr}[\mathcal{P}(K, q_c)\hat{\mathcal{O}}(q_c)]$ become poor. It is well known that there are IR divergences in the color-singlet state contributions for the inclusive P-wave charmonia decays [54,55], and these IR divergences can be removed by considering higher-order contributions. While for the exclusive P-wave charmonia decays, the same IR divergences always do not appear. However, as pointed out in Refs. [56,57], the higher-order contributions, such as the higher Fock-state contributions and the relativistic corrections, are still important to the exclusive P-wave charmonia decays. It indicates that the nonperturbative effects beyond those contained in $R'_{h_c}(0)$ may also play an important role in the radiative decays $h_c \to \gamma\eta^{(\prime)}$, even though the results with the zero-binding approximation for these decays are IR safe. Within a B-S equation approach, we would revisit the decays $h_c \to \gamma\eta^{(\prime)}$ by retaining the relative momentum q_c in the hard-scattering amplitude (i.e., the relativistic corrections), and this work is under way.

ACKNOWLEDGMENTS

This work is supported by the National Natural Science Foundation of China under Grants No. 11675061, No. 11775092, and No. 11435003.

APPENDIX: THE EXPRESSIONS OF 11 NUMERATORS n_i ($i = 1\sim 11$)

The expressions of the numerators n_i read

$$
\begin{aligned}
n_1 &= \frac{64M^2\xi^2}{(1-\xi^2)(1-x^2\xi^2)}((1-3x)l^2 + 2(1+x)l\cdot k - (1+x)M^2),\\
n_2 &= -16M^2\left\{\left(\frac{1-2x}{x(1-\xi^2)} - \frac{x(1-\xi^2)+4(1-x)}{x(1-\xi^2)(1-x^2\xi^2)}\right)l^2 - \frac{4l\cdot p[xl\cdot k-(1-x)l\cdot p]}{(1-x)^2M^2}\right.\\
&\quad - \frac{2}{(1-x)^2}\left(2x^2 - \frac{2x(x\xi^2+2)}{1-x^2\xi^2} + \frac{2x}{1-\xi^2} - \frac{3\xi^2(1-x^4)}{(1-\xi^2)(1-x^2\xi^2)}\right)l\cdot k\\
&\quad \left. - 2\left(\frac{2x\xi^2}{(1-x)(1-\xi^2)} - \frac{x^2\xi^2}{1-x^2\xi^2}\right)l\cdot p + \left(\frac{x\xi^2}{1-\xi^2} + \frac{x^2\xi^2}{1-x^2\xi^2}\right)M^2\right\},\\
n_3 &= -16M^2\left\{\left(\frac{1-2x}{x(1-\xi^2)} - \frac{x(1-\xi^2)+4(1-x)}{x(1-\xi^2)(1-x^2\xi^2)}\right)l^2 + \frac{4l\cdot p[xl\cdot k-(1-x)l\cdot p]}{(1-x)^2M^2}\right.\\
&\quad - \frac{2}{(1-x)^2}\left(4x-1+\frac{2x-3}{1-\xi^2} - \frac{2x^2(1-x^2\xi^4)+x^2\xi^2(\xi^2-x^2)}{(1-\xi^2)(1-x^2\xi^2)}\right)l\cdot k\\
&\quad \left. - 2\left(\frac{2x\xi^2}{(1-x)(1-\xi^2)} + \frac{x^2\xi^2}{1-x^2\xi^2}\right)l\cdot p + \left(\frac{x\xi^2}{1-\xi^2} + \frac{x^2\xi^2}{1-x^2\xi^2}\right)M^2\right\},
\end{aligned}
$$

$$n_4 = -\frac{32M^2(1+x\xi^2)}{(1-\xi^2)(1-x^2\xi^2)}\left(\frac{1-3x}{1+x}l^2 + \frac{2(1-3x)}{1-x}l\cdot k - 2l\cdot p - M^2\right),$$

$$n_5 = -\frac{32M^2(1+x\xi^2)}{(1-\xi^2)(1-x^2\xi^2)}\left(\frac{1-3x}{1+x}l^2 + \frac{2(1+x)}{1-x}l\cdot k + 2l\cdot p - M^2\right),$$

$$n_6 = -\frac{32M^2}{1-\xi^2}\left(\frac{2x^2+x+3}{x(1+x)}l^2 - \frac{6x^2-4x+6}{(1-x)^2}l\cdot k + \frac{4x}{1-x}l\cdot p - xM^2\right),$$

$$n_7 = \frac{64\xi}{(1-\xi^2)(1-x^2\xi^2)^2}((x^2\xi^2+2x\xi^2+1)l\cdot p + 4x\xi M^2),$$

$$n_8 = \frac{16}{1-x}\left\{2l\cdot k + \left(\frac{4(1-x)}{(1-x^2\xi^2)^2} + \frac{2x(1-x\xi^2)}{1-x^2\xi^2}\right)l\cdot p + \left(\frac{10x-4\xi^2}{(1-\xi^2)(1-x^2\xi^2)} + \frac{(x^4\xi^4-3x\xi^2-11x+1)(1-x\xi^2)}{(1-\xi^2)(1-x^2\xi^2)^2} + \frac{x^3\xi^2(2x^2\xi^2+3x\xi^2+1)}{(1-x^2\xi^2)^2}\right)M^2\right\},$$

$$n_9 = -\frac{16}{1-x}\left\{2l\cdot k + \left(\frac{4(1-x)}{(1-x^2\xi^2)^2} + \frac{2x(1-x\xi^2)}{1-x^2\xi^2}\right)l\cdot p - \left(\frac{x^2\xi^2(x^2\xi^2+2x+15)}{(1-x^2\xi^2)^2} - \frac{10x^2\xi^2(x-\xi^2)+6x\xi^2(1-x\xi^2)}{(1-\xi^2)(1-x^2\xi^2)^2} + \frac{x^3\xi^4-x^2\xi^2-2\xi^2+x-1}{(1-\xi^2)(1-x^2\xi^2)}\right)M^2\right\},$$

$$n_{10} = -\frac{64(x^2\xi^2+2x\xi^2+1)}{(1-\xi^2)(1-x^2\xi^2)^2}l\cdot p - \frac{128x}{(1+x)^2}\left(\frac{2(1+x)(1+x\xi^2)}{(1-\xi^2)(1-x^2\xi^2)^2} - \frac{x}{1-x^2\xi^2}\right)M^2,$$

$$n_{11} = \frac{32M^2(x^3+x^2+11x+3)}{(1-x)(1+x)^2(1-\xi^2)}. \tag{A1}$$

[1] J. P. Ma, Phys. Rev. D **65**, 097506 (2002).
[2] Y.-D. Yang, arXiv:hep-ph/0404018.
[3] G. Li, T. Li, X.-Q. Li, W.-G. Ma, and S.-M. Zhao, Nucl. Phys. **B727**, 301 (2005).
[4] B. A. Li, Phys. Rev. D **77**, 097502 (2008).
[5] J.-K. He and Y.-D. Yang, Nucl. Phys. **B943**, 114627 (2019).
[6] J. M. Gérard and E. Kou, Phys. Lett. B **616**, 85 (2005).
[7] Q. Zhao, Phys. Lett. B **697**, 52 (2011).
[8] J.-M. Gérard and A. Martini, Phys. Lett. B **730**, 264 (2014).
[9] R. Escribano, P. Masjuan, and P. Sanchez-Puertas, Phys. Rev. D **89**, 034014 (2014).
[10] T. Feldmann, P. Kroll, and B. Stech, Phys. Rev. D **58**, 114006 (1998).
[11] M. Ablikim *et al.* (BESIII Collaboration), Phys. Rev. Lett. **116**, 251802 (2016).
[12] M. Tanabashi *et al.* (Particle Data Group), Phys. Rev. D **98**, 030001 (2018).
[13] R. Zhu and J.-P. Dai, Phys. Rev. D **94**, 094034 (2016).
[14] Q. Wu, G. Li, and Y. Zhang, Eur. Phys. J. C **77**, 336 (2017).
[15] W. Buchmuller and S. H. H. Tye, Phys. Rev. D **24**, 132 (1981).
[16] E. J. Eichten and C. Quigg, Phys. Rev. D **52**, 1726 (1995).
[17] G. T. Bodwin, E. Braaten, and G. P. Lepage, Phys. Rev. D **51**, 1125 (1995); **55**, 5853(E) (1997).
[18] A. Ali and Ya. Parkhomenko, Phys. Rev. D **65**, 074020 (2002).
[19] T. Appelquist and H. D. Politzer, Phys. Rev. Lett. **34**, 43 (1975).
[20] A. De Rújula and S. L. Glashow, Phys. Rev. Lett. **34**, 46 (1975).
[21] R. Barbieri, R. Gatto, and R. Kögerler, Phys. Lett. B **60**, 183 (1976).
[22] V. A. Novikov, L. B. Okun, M. A. Shifman, A. I. Vainshtein, M. B. Voloshin, and V. I. Zakharov, Phys. Rep. **41**, 1 (1978).
[23] R. Barbieri, E. d'Emilio, G. Curci, and E. Remiddi, Nucl. Phys. **B154**, 535 (1979).
[24] P. B. Mackenzie and G. P. Lepage, Phys. Rev. Lett. **47**, 1244 (1981).
[25] J. G. Körner, J. H. Kühn, M. Krammer, and H. Schneider, Nucl. Phys. **B229**, 115 (1983).
[26] J. H. Kühn, Phys. Lett. B **127**, 257 (1983).
[27] P. Kroll and K. Passek-Kumerički, Phys. Rev. D **67**, 054017 (2003).
[28] V. N. Baier and A. G. Grozin, Nucl. Phys. **B192**, 476 (1981).
[29] B. Guberina and J. H. Kühn, Lett. Nuovo Cimento **32**, 295 (1981).

[30] J. H. Kühn, J. Kaplan, and E. G. O. Safiani, Nucl. Phys. **B157**, 125 (1979).
[31] B. Guberina, J. H. Kühn, R. D. Peccei, and R. Rückl, Nucl. Phys. **B174**, 317 (1980).
[32] P. Ball and G. W. Jones, J. High Energy Phys. 08 (2007) 025.
[33] V. L. Chernyak and A. R. Zhitnitsky, Phys. Rep. **112**, 173 (1984).
[34] T. Muta and M.-Z. Yang, Phys. Rev. D **61**, 054007 (2000).
[35] M.-Z. Yang and Y.-D. Yang, Nucl. Phys. **B609**, 469 (2001).
[36] S. S. Agaev, V. M. Braun, N. Offen, F. A. Porkert, and A. Schäfer, Phys. Rev. D **90**, 074019 (2014).
[37] S. Dittmaier, Nucl. Phys. **B675**, 447 (2003).
[38] G. 't Hooft and M. J. G. Veltman, Nucl. Phys. **B153**, 365 (1979).
[39] H. H. Patel, Comput. Phys. Commun. **197**, 276 (2015).
[40] H. H. Patel, Comput. Phys. Commun. **218**, 66 (2017).
[41] S. Alte, M. König, and M. Neubert, J. High Energy Phys. 02 (2016) 162.
[42] E. Eichten, K. Gottfried, T. Kinoshita, K. D. Lane, and T.-M. Yan, Phys. Rev. D **17**, 3090 (1978); **21**, 313(E) (1980).
[43] E. Eichten, K. Gottfried, T. Kinoshita, K. D. Lane, and T.-M. Yan, Phys. Rev. D **21**, 203 (1980).
[44] T. Feldmann, P. Kroll, and B. Stech, Phys. Lett. B **449**, 339 (1999).
[45] T. Feldmann, Int. J. Mod. Phys. A **15**, 159 (2000).
[46] R. Escribano and J.-M. Frère, J. High Energy Phys. 06 (2005) 029.
[47] R. Escribano and J. Nadal, J. High Energy Phys. 05 (2007) 006.
[48] F.-G. Cao, Phys. Rev. D **85**, 057501 (2012).
[49] B. Aubert *et al.* (*BABAR* Collaboration), Phys. Rev. D **74**, 012002 (2006).
[50] M. Ablikim *et al.* (BESIII Collaboration), Phys. Rev. D **86**, 092009 (2012).
[51] D. Babusci *et al.* (KLOE-2 Collaboration), J. High Energy Phys. 01 (2013) 119.
[52] E. B. Gregory, A. C. Irving, C. M. Richards, and C. McNeile (UKQCD Collaboration), Phys. Rev. D **86**, 014504 (2012).
[53] K. Ottnad and C. Urbach (ETM Collaboration), Phys. Rev. D **97**, 054508 (2018).
[54] R. Barbieri, R. Gatto, and E. Remiddi, Phys. Lett. B **61**, 465 (1976).
[55] G. T. Bodwin, E. Braaten, and G. P. Lepage, Phys. Rev. D **46**, R1914 (1992).
[56] P. Kroll, Nucl. Phys. B, Proc. Suppl. **64**, 456 (1998).
[57] S. M. H. Wong, Nucl. Phys. B, Proc. Suppl. **74**, 231 (1999).